World Academy of Science, Engineering and Technology
International Journal of Chemical and Molecular Engineering
Vol:4, No:5, 2010

Characteristics of Suspended Solids Removal by Electrocoagulation

C. Phalakornkule*, W. Worachai, T. Satitayut

Abstract**—**The electrochemical coagulation of a kaolin suspension was investigated at the currents of 0.06, 0.12, 0.22, 0.44, 0.85 A (corresponding to 0.68, 1.36, 2.50, 5.00, 9.66 $mA \cdot cm^{-2}$, respectively) for the contact time of 5, 10, 20, 30, and 50 min. The TSS removal efficiency at currents of 0.06 A, 0.12 A and 0.22 A increased with the amount of iron generated by the sacrificial anode, while the removal efficiencies did not increase proportionally with the amount of iron generated at the currents of 0.44 and 0.85 A, where electroflotation was clearly observed. Zeta potential measurement illustrated the presence of the highly positive charged particles created by sorption of highly charged polymeric metal hydroxyl species onto the negative surface charged kaolin particles at both low and high applied currents. The disappearance of the individual peaks after certain contact times indicated the attraction between these positive and negative charged particles causing agglomeration. It was concluded that charge neutralization of the individual species was not the only mechanism operating in the electrocoagulation process at any current level, but electrostatic attraction was likely to co-operate or mainly operate.

Keywords**—** Coagulation, Electrocoagulation, Electrostatics, Suspended solids, Zeta potential

I. Introduction

ELECTROCOAGULATION is an electrochemical technique whereby anodes (aluminium or iron electrodes) corrode to release active coagulants into solution. It is an alternative technology for wastewater treatment and recovery of valuable chemicals from wastewater. The main advantages of electrocoagulation over other conventional techniques such as chemical coagulation and adsorption are "*in situ*" delivery of reactive agents and compactness. Many studies have reported the potentials of electrocoagulation in treating a variety of wastewater including removing suspended solids [1, 2, 3], removing dyes [4, 5], heavy metals [6, 7], breaking oil emulsions in water [8, 9], removing complex organics [10, 11], removing bacteria, viruses and cysts [12].

However, despite of a number of discussions on the theory of electrocoagulation, there is a subjective that electrocoagulation is basically chemical dosing, with the only difference being the way in which the coagulant is delivered. A number of studies pointed out differences that in the case of electrocoagulation, the coagulants produced by the electrolytic oxidation were in the form of both monomeric hydroxide ions and highly charged polymeric metal hydroxyl species, e.g. $Fe(H_2O)_6^{3+}$, $Fe(H_2O)_5(OH)^{2+}$, $Fe(H_2O)_4(OH)_2^{+}$, $Fe_2(H_2O)_8(OH)_2^{4+}$ and $Fe_2(H_2O)_6(OH)_4^{4+}$, for anodes made of iron, and $Al_2(OH)_2^{4+}$, $Al_3(OH)_4^{5+}$ and $Al_{13}O_4(OH)_{24}^{7+}$, for anodes made of aluminum. The latter were formed due to the hydrolysis of metal ions [13, 14]. These species were believed to neutralize the electrostatic charges on the suspended solids and to facilitate agglomeration [2, 13, 14, 15]. In addition to the highly charged polymeric metal hydroxyl species, the amorphous solid metal hydroxide flocs could form at high metal ion concentrations and cause sweep-floc coagulation during settling [16, 2]. The destabilization mechanism of the contaminants, particulate suspension and breaking of emulsions have been described in broad steps as summarized by Mollah, et al. [13, 14]:

1. Compression of the diffuse double layer around the charged species by the interactions of ions generated by oxidation of the sacrificial anode.
2. Charge neutralization of the ionic species present in wastewater by counter ions produced by the electrochemical dissolution of the sacrificial anode. These counter ions reduce the electrostatic interparticle repulsion to the extent that the van der Waals attraction predominates, thus causing coagulation. A zero net charge results in the process.
3. Floc formation - the floc formed as a result of coagulation creates a sludge blanket that entraps and bridges colloidal particles still remaining in the aqueous medium.
4.

In order to further investigate the mechanistic difference between electrocoagulation and chemical coagulation and to clarify the broad steps stated in the related literature, this study investigated the differences following changes in zeta potential peaks during two processes. The system under investigation was suspended kaolin. The differences in zeta potential peaks during the two processes suggested the differences in mechanisms of the two processes. As will be illustrated, while chemical coagulation led to charge neutralization of individual species, electrocoagulation might lead to adsorption of highly charged polymeric metal hydroxyl species on to the colloids, which in turn create highly positive charged particles. These positive charged particles could attract the negative charged colloids, causing agglomeration.

C. Phalakornkule is with the Research and Technology Center for Renewable Products and Energy, and Department of Chemical Engineering, King Mongkut's University of Technology North Bangkok, Bangkok, 10800 Thailand (corresponding author to provide phone: +662-246-3253; fax: +662-587-0024; e-mail: cphalak21@yahoo.com; cpk@kmutnb.ac.th

W. Worachai is with the Department of Chemical Engineering, Bangkok, 10800 Thailand

T. Satitayut is with the Department of Chemical Engineering, Bangkok, 10800 Thailand

II. Materials and Method

A. Materials

The synthetic wastewater used in this study was a suspension of kaolin (Fluka Chemika 60609) at a concentration of 500 mg·L^{-1}. NaCl was added to the wastewater at a concentration of 2.3 g·L^{-1} to increase water conductivity. Table 1 presents the characteristics of the synthetic wastewater used in this study.

TABLE I CHARACTERISTICS OF SYNTHETIC WASTEWATER USED IN THIS STUDY

Parameters	Values
TSS (mg·L^{-1})	500
Turbidity (NTU)	480
Total COD (mg·L^{-1})	56500
NaCl (mg·L^{-1})	2340
Conductivity (mS·cm^{-1})	4.47
pH	6.03

B. Experiment

The electrochemical cell setup (Fig. 1) and the investigated conditions followed those of Bukhari [2]. The unit was composed of two stainless steel electrodes, a DC power source, a rheostat, an ammeter, a 2-L beaker with polyacrylic strips attached to the inside and a magnetic bar stirrer. Each stainless steel electrode had a dimension of 4 cm (width) x 18 cm (length) x 0.08 cm (thick) and an active surface area (the part submerged in liquid) of 88 cm^2. The stainless steel electrode composition was Fe > 66%, C < 0.08%, Cr 17.5-20%, Ni 8-11%, Mn < 2%, Si < 1%, P < 0.045%, S < 0.03%. The electrodes were 3 cm apart.

Experiments were carried out in a batch mode with a liquid sample of 1.2 L. Five different current intensities were applied (0.06, 0.12, 0.22, 0.44, 0.85 A corresponding to current density of 0.68, 1.36, 2.50, 5.00, 9.66 mA·cm^{-2}, respectively). For each current, contact times of 5, 10, 20, 30, and 50 min were used. At a certain contact time, a portion was pipetted from the middle of the beaker for zeta potential measurement. After experiencing the specified contact time, the sample was then taken to a standard jar test apparatus. After continuous mixing at 100 rpm for 1 min and at 30 rpm for 20 min, respectively, it was allowed to stand at room temperature for 20 min and a supernatant was then pipetted from the middle of the supernatant portion for the analysis of total suspended solids (TSS), turbidity, and Chemical Oxygen Demand (COD).

In order to compare the effectiveness of electrocoagulation and chemical coagulation, the same experimental system was setup, except this time the reactive reagent was provided to a system by dosing $FeSO_4^{2-}$ at the equivalent amount of iron generated by the electrolytic oxidation of the anode material according to Faradays' law:

$$w = \frac{I \cdot t \cdot M}{Z \cdot F} \quad (1)$$

where w is the iron dissolved (g); I is the current (A); t is the contact time (s); M is the molecular weight of Fe (M = 55.85); Z is the number of electrons involved in the redox reaction (Z=2); and F is the Faraday's constant (96500 C ·mol^{-1} of electrons).

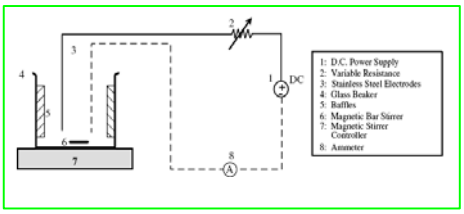

Fig. 1 Experimental system

Table 2 shows the amount of generated iron calculated according to Eq. 1. The pH of the chemical coagulation system was adjusted to the same values as in the electrocoagulation system using laboratory-grade sodium hydroxide (NaOH).

TABLE II. AMOUNT OF IRON GENERATED AT VARIOUS CURRENTS AND CONTACT TIMES ACCORDING TO FARADAY'S LAW

Contact time (min)	Iron generated (g)				
	I = 0.06 A	I = 0.12 A	I = 0.22 A	I = 0.44 A	I = 0.85 A
5	5.21x10^{-3}	1.041 x10^{-2}	0.0191	0.03820	0.07379
10	1.042 x10^{-2}	2.084 x10^{-2}	0.0382	0.07640	0.1476
20	2.084 x10^{-2}	4.167 x10^{-2}	0.0764	0.1528	0.2952
30	3.125 x10^{-2}	6.250 x10^{-2}	0.1146	0.2292	0.4427
50	5.209 x10^{-2}	1.042 x10^{-1}	0.1910	0.3820	0.7379

C. Analytical techniques

Zeta potentials were determined by Laser Doppler Electrophoresis (LDE) using a Malvern Zetasizer 3000 HS_A (Malvern Instruments Ltd., United Kingdom). LDE was the measurement of the colloidal particle movement when placed in an electric field. The measurement can be used to determine the sign of the charges on the particles and also their electrophoretic mobility. The temperature of the thermostated cell was kept at 25°C. The measured electrophoretic mobilities (U_E) were converted into zeta potentials (ζ) according to the Smoluchowski equation:

$$U_E = \varepsilon\zeta/\eta \quad (2)$$

The Smoluchowski equation applied when the salt concentration was high enough to significantly compress the double layer. The double layer thickness ($1/\kappa$) must be small compared to the particle diameter (a); $\kappa a >> 1$. The double layer thickness decreases rapidly with increasing ionic concentration. The viscosity (η) and dielectric constant (D, $\varepsilon=\varepsilon_o D$) of the suspending medium needed in the calculation were estimated from values of deionized water. Particle size measurement was also performed by Malvern Zetasizer 3000 HS_A based on the method of photon correlation. The turbidity of supernatant was determined using a Turbidimeter (model 6035, Jenway Ltd., United Kingdom). The pH was determined using a pH meter (model Lab 850, Schott, Germany).

Analyses of COD and TSS were according to the Standard Methods [17].

III. Results and Discussion

A. Total suspended solids, turbidity and COD removals

The relationship between the TSS, turbidity and COD removal efficiencies and contact time for the ranges of currents used are shown in Fig. 2a, b and c, respectively. The change in the TSS removal efficiency with contact time was similar to the change in the COD removal efficiency with contact time, while that of the turbidity removal efficiency was quite different. That is, the TSS and COD removal efficiencies increased with contact time for every current except during the first 10 and 20 mins at high currents of 0.44 and 0.85 A, respectively. At low residual suspended solid concentration occurring at high currents of 0.22 A, 0.44 A and 0.85 A, the turbidity measurement seemed not to be sensitive to small differences in the suspended solid concentration. Therefore, the TSS removal efficiency was selected for further discussion.

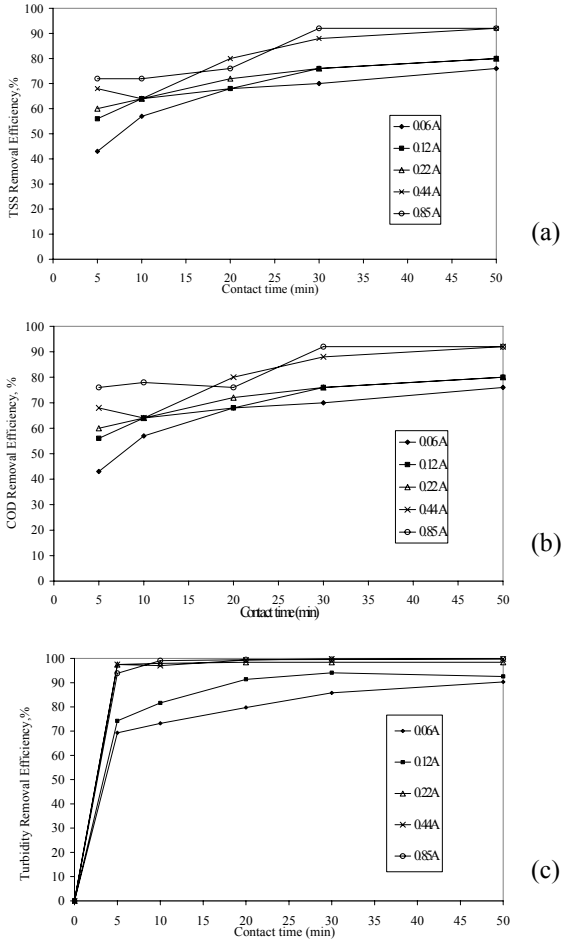

Fig. 2 The relationship between removal efficiencies and contact time for range of currents used in this study (a) TSS removal (b) turbidity removal (c) COD removal

Fig. 3 shows the TSS removal efficiency as a function of the amount of iron generated. The TSS removal efficiency at currents of 0.06 A, 0.12 A and 0.22 A increased with the amount of iron generated. Bukhari [2] reported similar results in his study and explained that the trend of suspended solids removal at lower currents of 0.05 A and 0.1 A were consistent with the charge neutralization mechanism, where removal increased as the coagulant dose increased. In contrast, sweep-floc coagulation was explained to occur at higher currents where the removal efficiencies did not increase proportionally with the amount of iron generated. For example, the TSS removal efficiencies were flat during the amount of iron generated between 70-300 mg-Fe at a high current of 0.85 A. Similar results were found by Holt et al. [15] where the turbidity reduction either remained stable or decreased when the condition facilitated metal hydroxide precipitation. In this study, the TSS removal efficiency increased again with the amount of iron generated between 440-740 mg-Fe at a high current of 0.85 A. In fact, during the condition at the high current, mechanisms involved could be quite complex. The metallic hydroxides were in the form of flocs, while the H_2 bubbles produced as a result of the redox reaction could cause the flotation of solid particles [13]. Holt et al. [15] observed the turbidity rise in the "no pollutant" case, due to metal hydroxide flocs originating from the electrocoagulation process and finally the establishment of a steady-state between the production and flotation of hydrolysed metal hydroxide flocs.

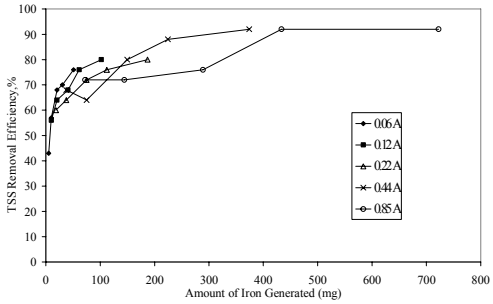

Fig. 3 TSS removal efficiency as a function of amount of iron generated for range of currents used in this study

B. Zeta potential measurement

Fig. 4a shows the zeta potential peak of the kaolin suspension before treatment, indicating the presence of negative surface charged particles. The zeta potential value of the system was -33 mV, indicating the system characteristics were moderately stable [18]. Fig. 4b shows the zeta potential peaks after passing a current of 0.06 A for 5 minutes. The peaks indicated the presence of both negative and positive surface charged particles. The zeta potential peaks of the samples collected between 5-20 mins at a current of 0.06 A also looked similar to Fig. 4b with a slight difference in the heights of the peaks and the positions on the x-axis (the zeta potential values). Fig. 4c shows the zeta potential peaks after passing a current of 0.06 A for 30 mins. Only one peak was observed and the net zeta potential was slightly positive (ζ = 13.1 mV), indicating the presence of slightly positive surface

charged particles. The zeta potential peaks of the samples collected during low mixing also looked similar to Fig. 4c.

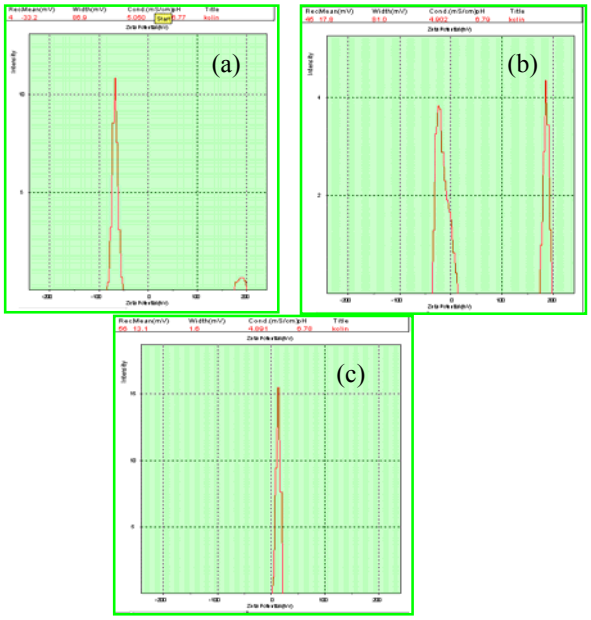

Fig. 4 Zeta potential of the colloidal system
(a) before passing the current
(b) subjected to a current of 0.06 A for 5 mins
(c) subjected to a current of 0.06 A for 30 mins

Fig. 5a shows again the zeta potential peak of the kaolin suspension before treatment, indicating the presence of negative surface charged particles. Fig. 5b shows the zeta potential peaks after passing a current of 0.85 A for 5 mins. Similar to Fig. 4b, the peaks indicated the presence of both negative and positive surface charged particles. The difference was that the peak at the negative zeta potential in Fig. 5b had significantly less intensity than that in Fig. 4b. Fig. 5c shows the zeta potential peaks after passing a current of 0.85 A for 30 mins. Only one peak was observed and the net zeta potential was slightly positive (ζ = 14.5 mV), indicating the presence of slightly positive surface charged particles. The zeta potential peaks of the samples collected between 5-20 mins at a current of 0.85 A also looked similar to Fig. 5c.

Zeta potential measurement based on the principle of electrophoretic mobility could detect particles in the range of 2-3000 nm. With electrocoagulation of the kaolin suspension, positive zeta potential peaks were observed even after passing the currents, either high or low, for a relatively short time. An experiment was performed to measure the zeta potential of the same system but without the presence of kaolin suspension. No such peaks were observed for any current and contact time. The data suggested that the highly positive charged particles were created by sorption of highly charged polymeric metal hydroxyl species onto the negative surface charged kaolin particles. The disappearance of the individual peaks after certain contact times indicated the attraction between these positive and negative charged particles, causing agglomeration without reducing the net surface charge of individual colloidal particles. However, the decreasing intensity and the shifting position toward zero zeta potential of the negative peaks indicated that a suppression of the electric double layer around the colloidal particles was also operating.

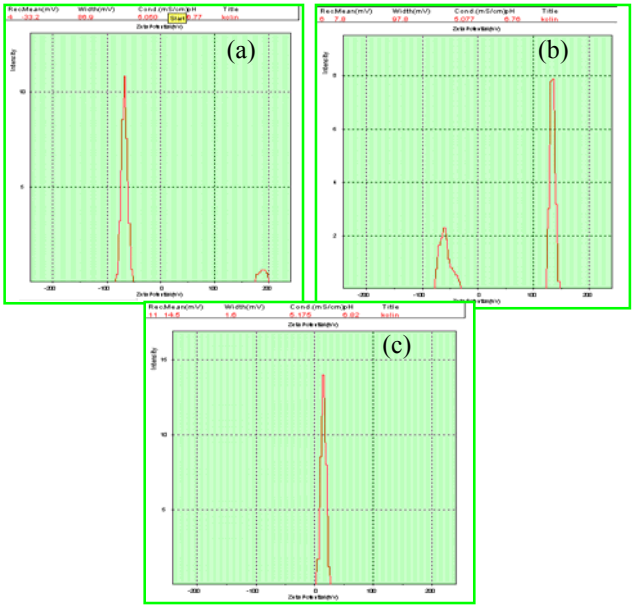

Fig. 5 Zeta potential of the colloidal system
(a) before passing the current
(b) subjected to a current of 0.85 A for 5 mins
(c) subjected to a current of 0.85 A for 30 mins

The change of zeta potential peaks from the chemical coagulation experiments was clearly different. Fig. 6a shows again the zeta potential peak of the kaolin suspension before treatment, indicating the presence of negative surface charged particles. Fig. 6b shows the zeta potential peak after Fe^{2+} dosing equivalent to the amount released by passing a current of 0.06 A for 5 mins. The amount of iron dosing calculated according to the Faraday's law is shown in Table 2. In contrast to Fig. 4b and 5b, only negative peak was observed. Compared to Fig. 6a, this peak was shifting toward zero zeta potential indicating the reduction in the net zeta potential. Fig. 6c shows the zeta potential peak after Fe^{2+} dosing equivalent to the amount released by passing a current of 0.06 A for 30 mins. The net zeta potential was -6 mV, indicating the strong agglomeration and precipitation as observed.

Fig. 7a, b and c show the zeta potential peak before treatment, after Fe^{2+} dosing equivalent to the amount released by passing a current of 0.85 A for 5 mins and after Fe^{2+} dosing equivalent to the amount released by passing a current of 0.85 A for 30 mins, respectively. These figures had similar appearances to Fig. 6a, b, and c except that with the higher iron dose, the net surface charge became positive (see Fig. 7c), corresponding to the observed threshold of destabilization.

As suggested by the theory and the observed zeta potential peaks in Fig. 6 and 7, iron coagulants suppressed the electric double layer around the colloidal particles, encouraging aggregation of the particles by van der Waals forces. The most effective removal corresponded to the isoelectric point with the iron dosing between 70-150 mg-Fe for the system of 1.2 L

kaolin suspension. With the appropriate dosing amount, the absolute zeta potential of the system was around 5 mV, indicating strong agglomeration and precipitation were achieved.

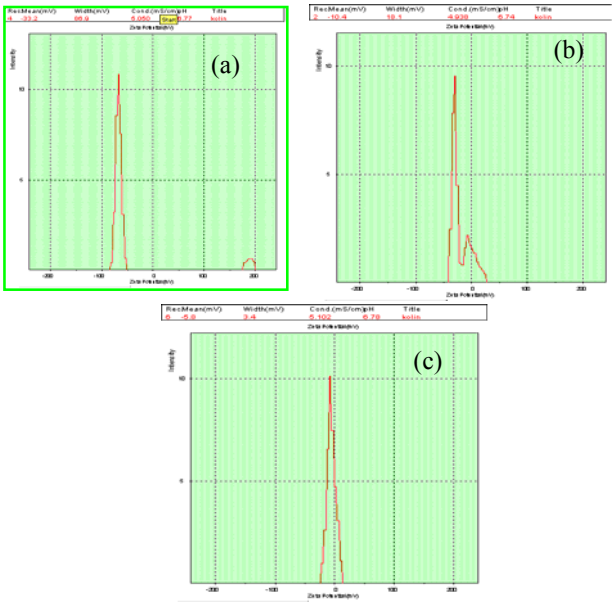

Fig. 6 Zeta potential of the colloidal system
(a) before chemical dosing
(b) subjected to Fe^{2+} dosing equivalent to the amount released by electrocoagulation at I = 0.06 A for 5 mins

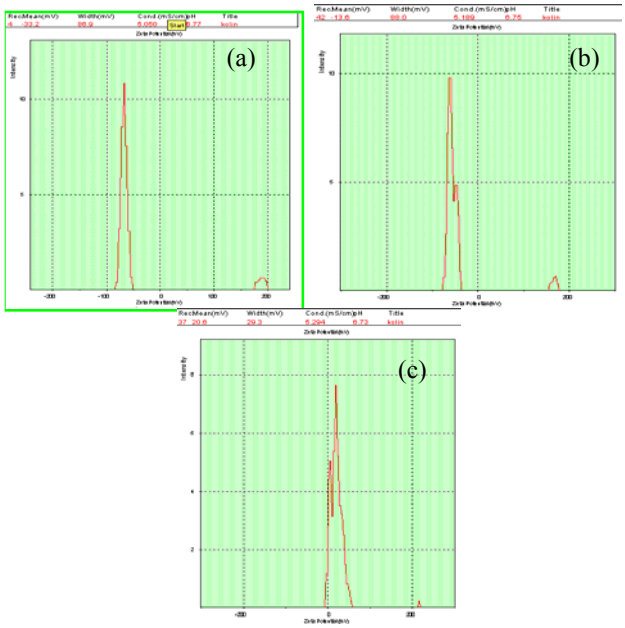

Fig. 7 Zeta potential of the colloidal system
(a) before chemical dosing
(b) subjected to Fe^{2+} dosing equivalent to the amount released by electrocoagulation at I = 0.85 A for 5 mins
(c) subjected to Fe^{2+} dosing equivalent to the amount released by electrocoagulation at I = 0.85 A for 30 mins

A number of earlier works investigated the change in absolute zeta potential during electrocoagulation, but not the individual peaks [2, 19], and most studies concluded that charge neutralization of the negative surface charged colloids (kaolin in this case) by counter ions (Fe^{2+} and Fe^{3+} in this case) produced by the electrochemical dissolution of the sacrificial anode. These counter ions reduced the electrostatic interparticle repulsion to the extent that the van der Waals attraction predominated, thus causing coagulation. A zero net charge resulted in the process. However, in their study of comparison between chemical dosing and electrocoagulation in the system of clay suspension, Holt et al. [15] suggested that charge neutralization appeared implausible because the dominating aluminate ion was in the form of a negative aluminium ion, $Al(OH)_4^-$ (aq) at a pH of 8.5. However, no evidence of alternative mechanism was illustrated. In this study, the presence of highly positive charged species together with the presence of the original negative surface charged kaolin was observed. The final disappearance of both negative and positive charged particles suggested the interaction between these oppositely charged particles, i.e., these positive charged particles could attract negative charged colloids, causing agglomeration. Therefore, charge neutralization of the individual species was not the only mechanism operating in the electrocoagulation process at any current level, but electrostatic attraction was proved to co-operate or mainly operating.

C. Other characteristics of electrocoagulation

Fig. 8a shows the wastewater before treatment. Fig. 8b and c show the appearance of the system after passing a low current of 0.06 A and a high current of 0.85 A, respectively, for the same period of 30 minutes. The pictures clearly show that sedimentation occurred in Fig. 8b, while electroflotation occurred in Fig. 8c. Actually, in this study, electroflotation of the coagulated particles occurred at currents higher than 0.22 A. When the applied current was below this value, electroflotation was not observed regardless of how long the contact time was. Electroflotation was explained to depend on the H_2 bubbles density produced at the cathodes. A high current produces high bubble density resulting in a high upward momentum flux, while a low current produces low bubble density, leading to a low upward momentum flux and domination of sedimentation over flotation [15].

Another note is that the pH of the system was stable between 6.7-6.8 during electrocoagulation. The stabilization of the pH was previously reported to be a characteristic of the electrocoagulation reactor [15]. This could be explained by the production of OH^- at the cathode and its consumption at the anode at equal rates as shown in Mechanism I [20]:

Mechanism I

Anode:

$$Fe(s) \rightarrow Fe^{2+}_{(aq)} + 2e^- \quad (3)$$

$$Fe^{2+}_{(aq)} + 2OH^-_{(aq)} \rightarrow Fe(OH)_{2\,(s)} \quad (4)$$

Cathode:

$$2H_2O_{(l)} + 2e^- \rightarrow H_{2(g)} + 2OH^-_{(aq)} \quad (5)$$

Overall:

$$Fe_{(s)} + 2H_2O \rightarrow Fe(OH)_2(s) + H_2(g) \quad (6)$$

When the amount of iron in the water exceeds the solubility of the metal hydroxide, formation of the amorphous metal hydroxide could take place according to Mechanism II,

whose overall reaction does not change H^+ or OH^- concentration and thus does not change the pH of the system.

Mechanism II

Anode:

$$4Fe(s) \rightarrow 4Fe^{2+}_{(aq)} + 8e^- \quad (7)$$

$$4Fe^{2+}_{(aq)} + 10H_2O_{(l)} + O_{2(g)} \rightarrow 4Fe(OH)_{3(s)} + 8H^+_{(aq)} \quad (8)$$

Cathode:

$$8H^+_{(aq)} + 8e^- \rightarrow 4H_{2(g)} \quad (9)$$

Overall:

$$4Fe_{(s)} + 10H_2O_{(l)} + O_{2(g)} \rightarrow 4Fe(OH)_{3(s)} + 4H_{2(g)} \quad (10)$$

However, the stabilization of the pH does not occur in every electrocoagulation reactor as previously reported by Holt et al. [15]. For example, Drogui et al. [21] observed significant pH rises when treating agro-industry wastewater using iron and aluminum as anodes. The increase in pH during electrocoagulation was primarily attributed to the increase of hydroxide ions in the solution resulting from water reduction at the cathode (Eq. 5), while the reaction consuming hydroxide ions to produce ferrous hydroxide (Eq. 4) was less substantial.

The final note is on the surface deterioration of the anode. As shown in Fig. 9, the release of iron from the surface was not distributed over the entire plate, but concentrated on certain areas resulting in holes with a size of approximately 10^1-10^2 microns. Particles and microorganisms in the wastewater could be trapped inside these holes and could obstruct the release of metal ions. Therefore, the design of clean-in-place of anodes is one of the main challenges for electrocoagulation technology.

(a) (b) (c)

Fig. 8 Photos of kaolin suspension
(a) no treatment
(b) subjected to electrocoagulation at I = 0.06 A for 30 mins
(c) subjected to electrocoagulation at I = 0.85 A for 30 mins

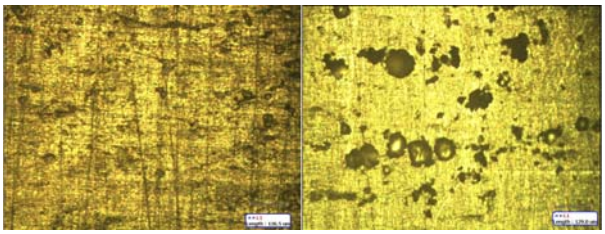

(a) (b)

Fig. 9 Photos of anode
(a) before and (b) after electrocoagulation experiments

IV. Conclusion

The main conclusion of this study was that charge neutralization of the individual species was not the only mechanism operating in the electrocoagulation process at any current levels, but electrostatic attraction was likely to co-operate or mainly operate. Zeta potential measurement illustrated the presence of highly positive charged particles presumably created by sorption of highly charged polymeric metal hydroxyl species onto the negative surface charged kaolin particles at both low and high applied currents. The disappearance of the individual peaks after certain contact times suggested the attraction between these positive and negative charged particles, causing agglomeration. The TSS removal efficiency at currents of 0.06 A, 0.12 A and 0.22 A increased with the amount of iron generated by the scarified anode, while the removal efficiencies did not increase proportionally with the amount of iron generated at currents of 0.44 and 0.85 A, where electroflotation was clearly observed. The particle size measurement of both chemical coagulation and electrocoagulation showed no significant difference in average particle size even though the result suggested different mechanisms responsible for reducing electrostatic repulsive forces. The explanation was that the measured particle sizes were of the floc formed by coagulation, the process following the reduction on electrostatic repulsive forces between particles.

References

[1] N.S. Abuzaid, A.A. Bukhari, Z.M. Al-Hamouz, J. Environ. Sci. Health, Part A 33, 7 (1998) 1341-1358.
[2] A. Bukhari, Bioresour. Technol. 99, 5 (2008) 914-921.
[3] M.J. Mattenson, R.L. Dobson, R.W. Glenn, W.H. Kukunoor, E.J. Clayfield, Colloids and Surfaces A: Physicochem. Eng. Aspects 104 (2005) 101-109.
[4] C.-L. Yang, J. McGarrahan, J. Harard. Mater. B127 (2005) 40-47.
[5] F. Zidane, P. Droguin, B. Lekhlif, J. Bensaid, J.-F. Blais, S. Belcadi, K. El kacemi, J. Hazard. Mater. 155, 1-2 (2007) 153-163.
[6] I. Heidmann, W. Calmano, J. Hazard. Mater. 152, 3 (2008) 934-941.
[7] N. Meunier, P. Drogui, C. Montané, R. Hausler, G. Mercier, J.-F. Blais J. Hazard. Mater. 137, 1 (2006) 581-590.
[8] K. Bensadok, S. Benammar, F. Lapicque, G. Nezzal, J. Hazard. Mater. 152, 1 (2008) 423-430.
[9] P. Cañizares, F. Martínez, C. Jiménez, C. Sáez, M.A. Rodrigo, J. Hazard. Mater. 151, 1 (2007) 44-51.
[10] M. Uğurlu, A. Gürses, Ç. Doğar, M. Yalçın, J. Environ. Manage. 87, 3 (2008) 420-428.
[11] Y.Ş. Yıldız, A.S. Koparal, B. Keskinler, Chem. Eng. J. 38, 1-3 (2008) 63-72.
[12] B. Zhu, D. A. Clifford, S. Chellam, Water Res. 39, 13 (2005) 3098-3108.
[13] M.Y.A. Mollah, R. Schennach, J.R. Parge, D.L. Cocke, J. Hazard. Mater. B84 (2001) 29-41.
[14] M.Y.A. Mollah, P. Morkovsky, J.A.G. Gomes, M. Kesmez, J. Parga, D.L. Cocke, J. Hazard. Mater., B114, 1-3 (2004) 199-210.
[15] P.K. Holt, G.W. Barton, M. Wark, C.A. Mitchell, Colloids and Surfaces A: Physicochem. Eng. Aspects 211 (2002) 233-248.
[16] L.D. Benefield, J.F. Judkins, B.L. Weand, Process Chemistry for Water and Wastewater Treatment, Prentice-Hall, Englewood Cliffs, N.J., 1982.
[17] American Public Health Association. Standard methods for the examination of water and wastewater. Washington, DC: American Public Health Association, American Public Association (APHA), 1998.
[18] R.J. Hunter, Zeta potential in colloid science. Principles and Applications. Academic press Inc., 1981.
[19] E. Ofir, Y. Oren, A. Adin, Desalination 204 (2007) 87-93.

[20] M.S. Farooqui, Combined Electrooxidation and Electrocoagulation Processes for the Treatment of Municipal Wastewater. Master Thesis. King Fahd University of Petroleum and Minerals, Saudi Arabia, 2004.
[21] P. Drogui, M. Asselin, S.K. Brar, H. Benmoussa, J.-F. Blais, Sep. Purif. Technol. 61 (2007) 301-310.